

Mission Design and Simulation Considerations for ADReS-A

Susanne Peters

Universität der Bundeswehr München

Roger Förstner

Universität der Bundeswehr München

Hauke Fiedler

Deutsches Zentrum für Luft- und Raumfahrt DLR

ABSTRACT

Space debris in general has become a major problem for modern space activities. Guidelines to mitigate the threat have been recommended, better prediction models are developed and an advanced observation of objects orbiting Earth is in progress. And still – without the implementation of active debris removal (ADR), the number of debris in space will exponentially increase. To support the ongoing research on ADR-missions, this paper presents the updated mission design of ADReS-A (Autonomous Debris Removal Satellite - #A) - one possible concept for the multiple active removal of large debris in Low Earth orbit, in this case especially of rocket bodies of the SL-8-type. ADReS-A as chaser satellite is supported by at least 5 de-orbit kits, allowing for the same number of targets to be removed. While ADReS-A is conceived for handling of the target, the kit's task is the controlled re-entry of the designated rocket body.

The presented mission design forms the basis for the simulation environment in progress. The simulation shall serve as testbed to test multiple scenarios in terms of approach and abort optimization or different tumbling modes of the target. The ultimate goal is the test of autonomous behaviors of the spacecraft in case of unforeseen failures during the approach phase. Considerations to create a simulation for the described mission are presented and discussed. A first visualization of pre-calculated aboard trajectories can be found at the end of this paper.

1. INTRODUCTION

Sending satellites into Space has increased the standard of modern live immensely – Earth observation, weather forecast and an increased range for data transfer are just a few positive outcomes to be named. Unfortunately, once in space, it is quite difficult to repair any failure or malfunction of a satellite. Battery discharge and propellant limitations add to a limited lifetime. So far, most satellites have been left in space to degrade, explode or collide with each other, leading to about 17.000 officially tracked objects in the Low Earth orbit in 2015. With this number increasing, active satellites have to perform more and more avoidance maneuver [1] - actions, that limit their mission time and propellant reserves. Moreover, they are endangered to collide with undetected objects and, thus, to become debris themselves. Besides the officially recommended mitigation guidelines on design and post mission disposal of modern satellite missions, active space debris removal needs to be encouraged to slow down the growing number of space debris.

Various ideas on removal missions have been proposed in the past with challenges often addressing the handling of the uncooperative target. Being in close vicinity, the spacecraft relies on its on-board sensors to calculate relative position and velocity. A flawless connection to ground control cannot be ensured and is, moreover, time consuming, which creates the need for high-level autonomy and on-board processing of the spacecraft.

The idea of implementing autonomy in spacecraft in general has been followed for some time, however, requirements for a specific implementation need to be derived from a mission architecture. This paper introduces the concept of an autonomous debris removal satellite (ADReS-A), its mission architecture and a first approach of how to simulate and visualize the rendezvous path of the satellite. Abort scenarios in case of a failure are also implemented. The simulation shall serve as a testbed for the autonomy and is based on the sensor data of ADReS-A, derived from the spacecraft preliminary design, presented briefly within this work.

2. MOTIVATION

The complex task of two objects performing a docking maneuver in space with not much more than communication contact to intervene the scenery from ground cannot be underestimated. It gets more complex if one of the objects is uncooperative – without any reflecting sensors, attachment feature or data about its attitude and motion. As active debris removal mirrors exactly the scenery of removing uncooperative objects, the idea of implementing self-awareness and with such high-level autonomy is a logic derivation. A broad range of verification and validation tests are required before the actual implementation need to be considered.

Software is usually tested at first through simulations. The challenge is to define beforehand, what the simulation should include. The presented work discusses different considerations, for example the level of accuracy needed, the part of the mission tested when designing a simulation, or general requirements such as the used optimization algorithms. The ADReS-A mission will serve as role model and is therefore is presented first.

3. MISSION DESIGN

3.1 Targets

There are about 17.000 officially catalogued space debris objects in space. Their sizes vary from a few centimeters to a few meters, masses show an according range, distributing from a few grams to a few tons. Additionally, smaller undetected objects orbit the Low Earth orbit (LEO). As a cascade effect has already been initiated according to various experts of the field [2], the task of slowing down this development should be of primary task. For a long-term stabilization of the environment, the source of the increase needs to be removed – large, massive objects orbiting in highly frequented orbits.

Top candidate-list are published by multiple authors [3], and even if they do not match each other 100%, they resemble on a lot of points. As removal missions will be required for many years, ADR-missions should be most effective, resulting for example in the requirement of removing more than one object per launch. Recommendations given by the experts state 5 to 15 large objects per year for a stabilization of the space environment.

For the scope of the ADReS-A mission, the two objectives - high priority target & 5 to 15 objects per launch - are combined. The outcome are SL-8 rocket bodies as most suitable targets for a multiple active debris removal mission [4]. With 292 objects of this same kind, spreading mainly within three different inclination ranges, as can be seen in Fig. 1, it is most likely for a possible removal mission to find a suitable amount of targets in close vicinity. A further advantage is the fact of similar geometry of the rocket bodies. The design of the removal technology can be simplified as it can concentrate on one profile rather than on multiple ones.

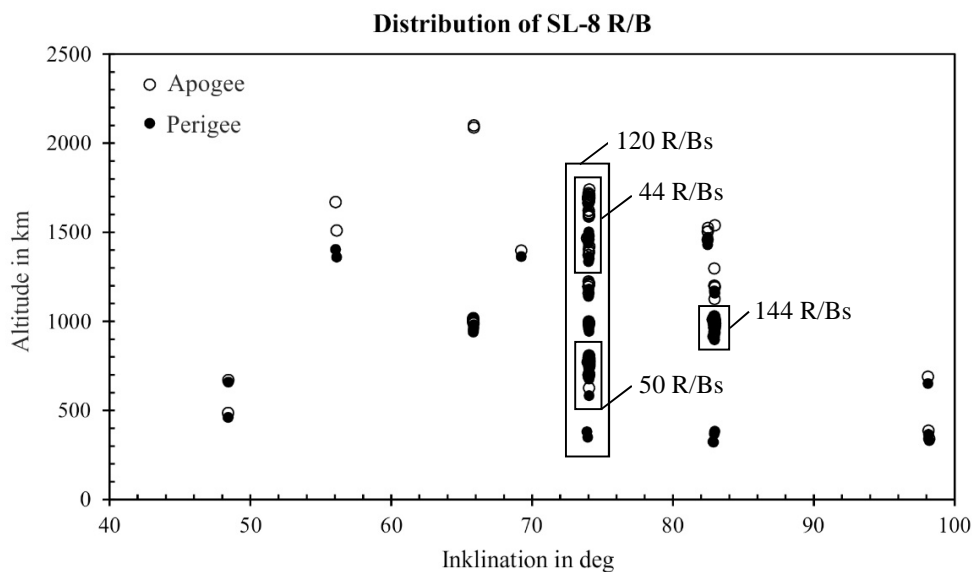


Fig. 1. Distribution of 292 SL-8 R/Bs over altitude and inclination as of 2014

3.2 Mission Architecture

With the requirement of one launcher for the removal of multiple objects, the question of controlled or uncontrolled re-entry arises. As objects with a mass of over a ton are not considered to be vaporize during the re-entry, at least part(s) of them will reach the Earth surface [5]. To avoid urban areas, and with the knowledge of quite a wide range for the break-up area, a controlled re-entry into an ocean should be aimed for.

The capture of debris in space is not considered to be simple. For ADReS-A, the mechanism of a robotic arm is in favor. Due to the close vicinity, quite a complex approach needs to be performed. With the aim for controlled de-orbit, ADReS-A will be supported by de-orbit kits that will perform the re-entry. This way, the system complexity can be focused within the main satellite, the kits can be designed somewhat simpler as they will vaporize during their passage through the atmosphere.

To limit deltaV requirements, the set-up will be launched into a parking orbit close to the targets one. ADReS-A is designed to carry one kit at a time, leaving the need to secure the others while they wait for their pick-up. The kits will therefore stay spin-stabilized in the parking orbit while ADReS-A shuttles between the targets and the kits. The required deltaV is calculated to about 15 m/s per orbit change, a successful close approach will take about 5 to 6 m/s per approach.

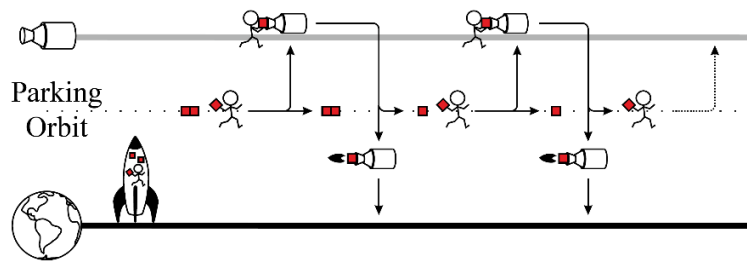


Fig. 2. Principle mission architecture, following [6]

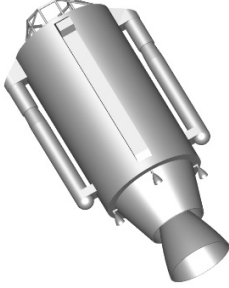
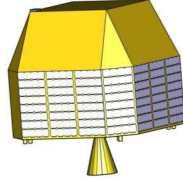
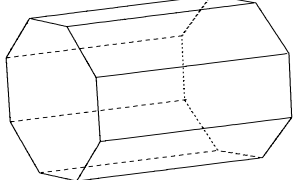
Data of the targets position will be obtained from the ground station, as their instruments allow for an accuracy of a few hundred meters [7]. The Visual Light Camera (VLC) used is able to detect the object in distances up to a few kilometer. Both values together allow for a safe determination of the target. The approach up to a distance of 25 m will be supported by the VLC, the final approach and determination of the tumbling rate will be supported by a Time of Flight Camera (ToFC). Reference [8] explains the various steps that are taken to determine the tumbling rate of the rocket body at changing distances. Once in a distance of 11 m, the actual capture of the target is initiated, including a berthing box and other safety margins explained later. The simulation of the approach trajectory starts at this distance and ends with either the capture or an abort due to emerging misconduct or failures.

3.3 Satellite Design

The satellite design has been specified to use data as accurate as possible to create a simulation with realistic background. While the design of the rocket body is fixed, the kit is conceptualized to fit into its nozzle. This connecting position was chosen, as the rocket main engines mechanical properties promise the flare to be the most stable one on the rocket. Additionally, it is aligned with the rockets center of mass, which allows for a limitation of the tumbling during deorbit. Following the description, the kit can be described as an advanced additional thruster. A clamp mechanism will hold the kit in its position during the procedure. ADReS-A in turn is designed to handle the target and the kit at once. It is therefore equipped with a robotic arm, able to grab the target and the kit. A second linear arm will hold the kit in position and eventually attach it to the rocket. Multiple thruster will ensure the satellites flexibility and the energy system is built to last for at least the time of the mission – 1 year. As for ADReS-A the autonomy is the key part, the on-board computer will be redundant. While the kit will work on liquid oxygen and liquid methane, ADReS-A is designed for hydrazine.

While the 3D design of the kit is settled, the more complex version of ADReS-A is close to its complementation. The system design is finished, while the 3D version is in progress to be derived from there. Tab. 1 gives an overview of the main data of the involved objects. As the rocket body of the SL-8 type did not empty their tank after end-of-life (EOL), the rockets are assumed to have 10 to 20% propellant is left in their tanks. The total mass of the kit and ADReS-A include a 15% margin.

Tab. 1. Overview of the main design data of the involved objects

	SL-8 Rocket Body	De-Orbit Kit	ADReS-A
			
Dry Mass	Ca. 1400 kg	Ca. 177 kg*	Ca. 645 kg*
Gross Mass	Ca. 1600 kg	Ca. 440 kg*	Ca. 999 kg*
Diameter	2.4 m	1.8 m	2.3 m
Length	6.5 m	1.8 m	3.0 m

* dry and gross mass include a 15% margin for kit and ADReS-A

4. SIMULATION

4.1 Considerations

Before a simulation is created, some kind of architecture needs to be designed to figure out the different parts involved, their interaction and yet unsolved problems that should be addressed. In case of the simulation for ADReS-A, the early architecture follows Fig. 3. Further improvement of the simulation will enlarge the architecture accordingly.

Considerations for simulations in general cover their features and/or promised capabilities. The ADReS-A simulation thus involves the parameters of the environment, the targets and spacecraft designs, performance capabilities and plans for the mission. Optimization tools are used for fuel efficiency. The used tool was developed and provide by Gerdts [9]. “It applies a robust SQP method combined with a gradient calculation using sensitivity DAEs and is suitable for optimal control problems subject to differential algebraic equations of index one.” [10]

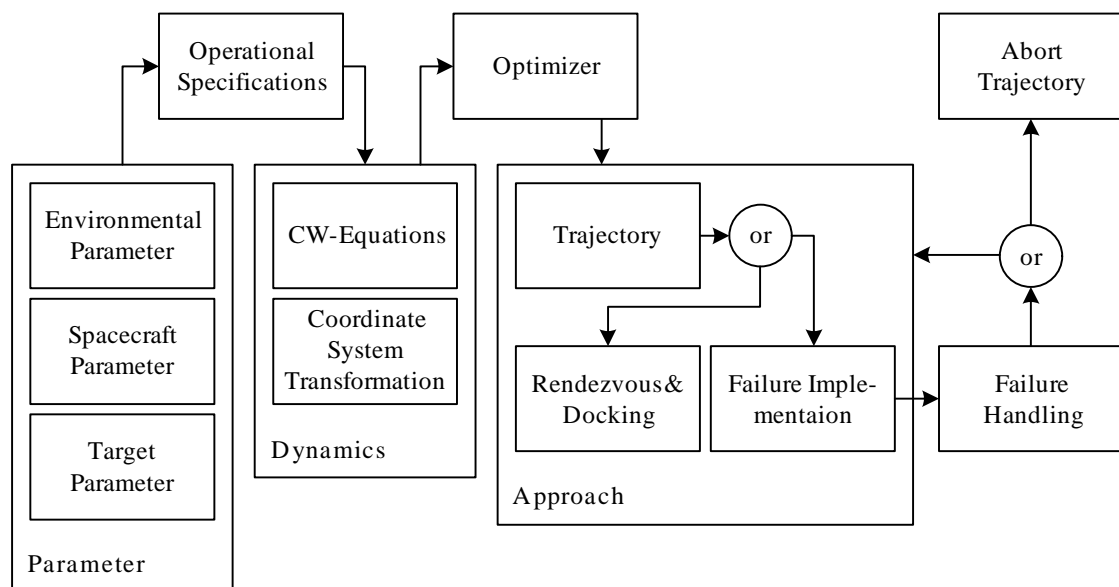


Fig. 3. Early Simulation Architecture ADReS-A.

Task

The actual task of the simulation in question is an accurate rendering of the approach trajectory combined with the implementation of a failure. The system then has to act accordingly, to its best knowledge and safety settings, to categorize the failure and decide if the approach is still doable or if an abort trajectory should be followed. It is assumed that ground control has no possibility to intervene during this process. Therefore, the system has to work on high level automation or autonomy, based on on-board processing.

Environment

As mentioned during the mission architecture, the active debris removal shall take place in LEO. With SL-8 R/B as chosen targets, the specific orbit of 970 km altitude and 82.9 deg inclination on a nearly circular orbit is simulated. The simulation addresses the actual approach. The objects – target and chaser-setup – have similar sizes and weight. Therefore perturbations will act similar on both systems. Proposed simplifications are listed further below. Other environmental influences like the sun illumination are addresses during the design phase of the satellite.

Operational Considerations

Tab. 1 contains the used geometry of the involved objects. For the simulation, the target and the ADReS-A-De-orbit Kit combination are approximated as cylinders (as can be seen in Fig. 4 of Chapter 4.2), the kit located on top of ADReS-A. Moreover, mass, propulsion capability and the moments of inertia derived from the preliminary 3D-model created are implemented.

The sensors for the spacecraft and kit system designs include cameras for the observation of the target – the VLC and the ToFC. As the simulation starts at a distance of about 11 m, mainly the data provided by the ToFC will give information about the tumbling mode and attitude of the rocket body [8]. At the time of writing, these data are taken as given attributes and shall be added in a later version of the simulation. The simulation as such shall be feed with the relative coordinates of the chaser set-up (ADReS-A & De-orbit Kit) and the target. Additionally, their relative velocity, and their respective angular velocities are provided. As mentioned before, the respective moments of inertia should be known as well as the intended docking points. The grabbing with the robotic arm will be performed while the chaser setup is in a berthing box. This box allows for the robotic arm to handle the object without the target and the chaser colliding. As the arm has limited range, the berthing box dimension should not exceed 2 m. Additional time available to follow the approach trajectory has to be specified. This way, the algorithm can optimize for fuel consumption.

The final approach will need to be performed during the assigned phases of a period (α_{Op} in Tab. 2). The figures displayed in Tab. 2 give an overview of the different phases of the assigned orbit. The instruments require sufficient sun illumination but do not allow for too bright illumination - the eclipse phase, direct sun and bright reflections of the target into the field of view of the camera are therefore excluded. This limits the actual time for operation to a few degrees (α_{Op}), in other words to 3092 s or about 52 min. As the used algorithm for movement prediction takes longer than that [8], multiple periods have to be run before the actual approach can be initiated.

Tab. 2. Different phases of one orbit

Illumination phase of orbit α_{Ill}		$\alpha_{Ill} \rightarrow 4131 \text{ s}$
Eclipse phase of orbit α_{Ecl}		$\alpha_{Ecl} \rightarrow 2099 \text{ s}$
Direct sun or too bright reflection - unfavorable for instruments $\alpha_{Sun}/\alpha_{Ref}$		$\alpha_{Sun+Ref} \rightarrow 1038 \text{ s}$
Potential phase for operation α_{Op}		$\alpha_{Op} \rightarrow 3093 \text{ s}$

Dynamics

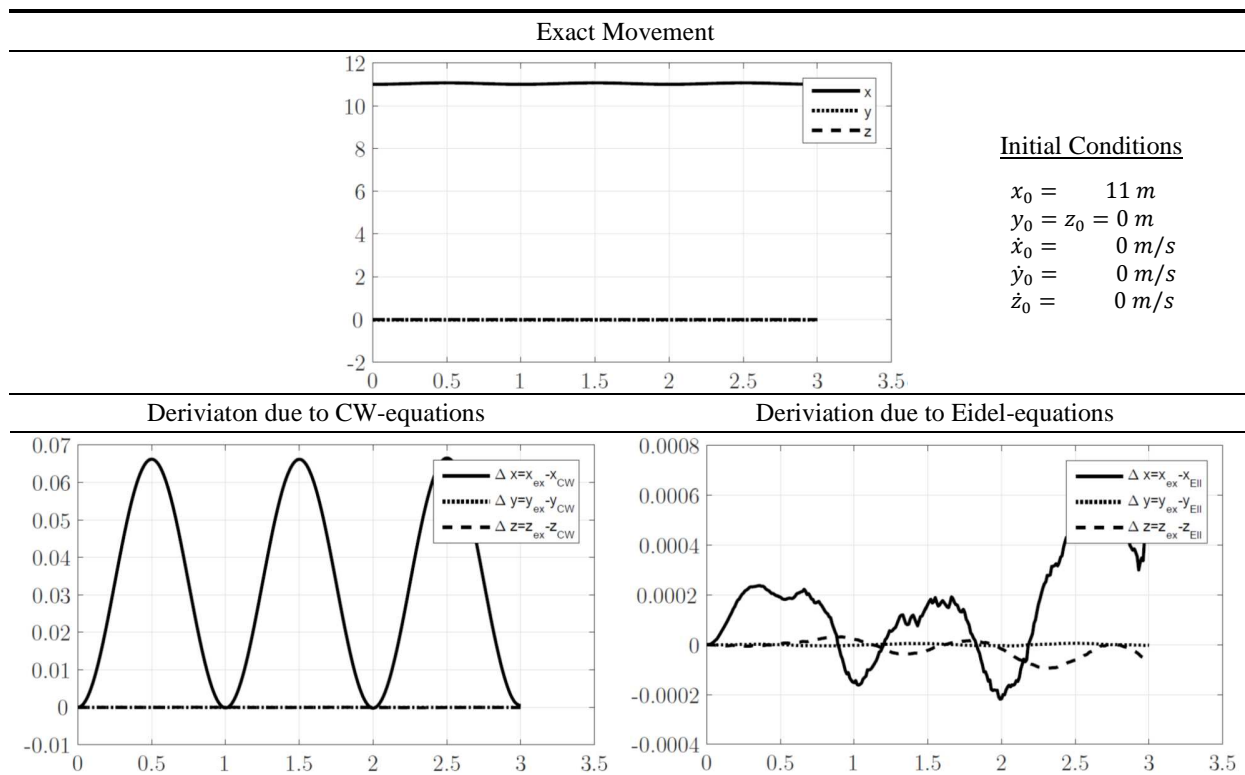
Flight dynamics in space are not as straight forward as on Earth. Objects move in three dimensions, all of them influencing each other at least slightly. Tab. 3 to Tab. 7 display the ‘Exact Movement’ of a chaser 11 m behind the target. The x-axes show the periods covered (up to 3 periods are displayed), the y-axes show the derivation from the original position in meter. For the displayed graphs titled ‘Derivation due to CW-equations’ and ‘Derivation due to Eidel-equations’, the y-axes show the derivation from the ‘Exact Movement’ in meter. While Tab. 3 graphs the movement and derivations due to the distance of target and chaser, Tab. 4 to Tab. 7 have a velocity added: Tab. 4 shows the movement with a small velocity in x-direction, Tab. 5 has a velocity in y-direction added, Tab. 6 shows how a velocity in the z-direction changes the relative position and Tab. 7 displays the overlaid velocities.

Each of the graphs shows three different lines - the straight line shows the x-direction (flight direction), the dashed line represents the movement in the z-direction (pointing away from Earth center), the dotted line presents the y-direction (complementing the system).

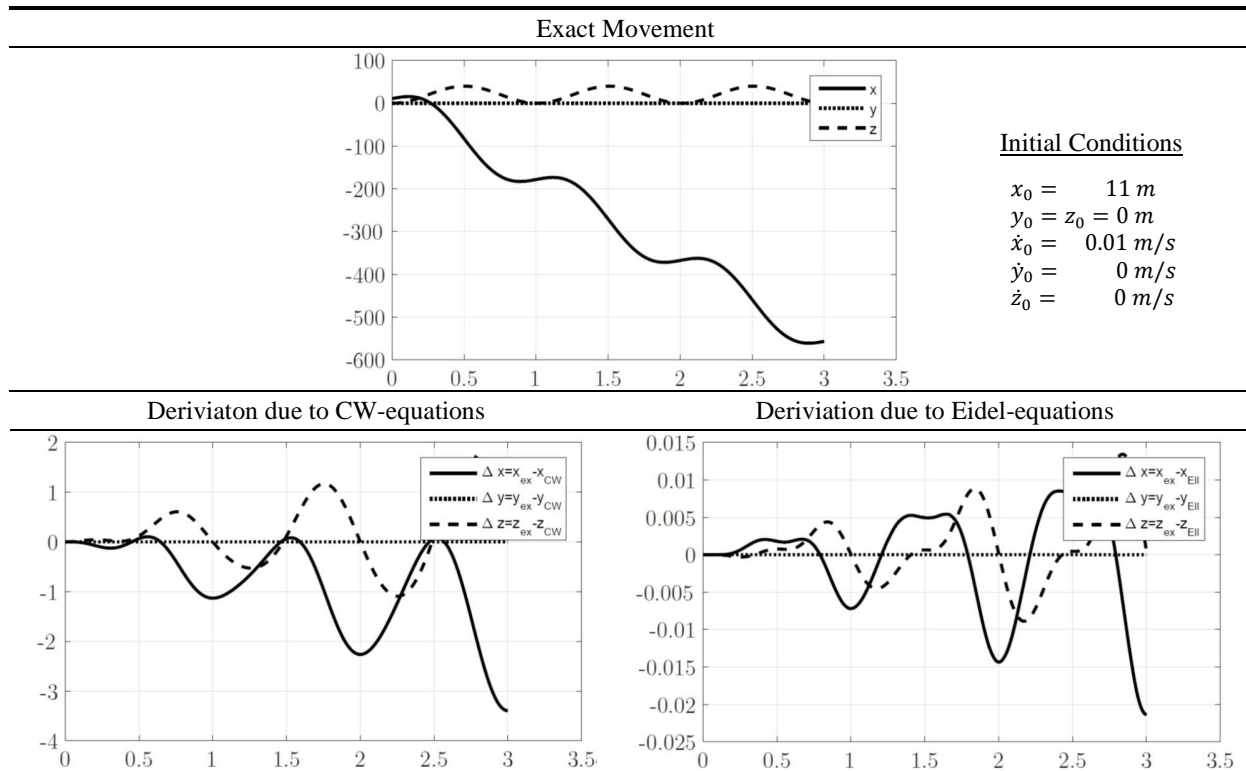
Calculations for the ‘Exact Movement’ have been performed numerically. The Clohessy-Wiltshire equations (CW-equations) and the Eidel-equations allow for an analytic view of the problem and are a good approximation of nearly similar orbits. They can be used for relative flight maneuvers for objects less than 100 m apart. The CW-equation deviations from the exact (numerical) data is titled ‘Derivation due to CW-equations’. The Eidel calculations performed by Eidel [11] are created for small elliptical orbits for eccentricities smaller than 0.1. As displayed in the graphs, they are in every direction more precise than the CW-calculations and do not differ from the exact values more than 0.02 m, considering the initial conditions listed. The according equations can be found in Reference [12]. Why they are not used for the created simulation is explained in the simplification part of this chapter.

Other dynamical issues, for example pointing requirements, should be listed but do not necessarily concern the final approach. Such requirements are the pointing of the solar panels towards the sun during recharge procedures, antennas pointing towards Earth during communication phases, ensuring that the sun does not meet any ‘forbidden area’ such as sensitive sensors and the fact that during the far and close approach the required sensors and cameras point towards the target, while avoiding direct sunlight if required (see α_{op} in Tab. 2).

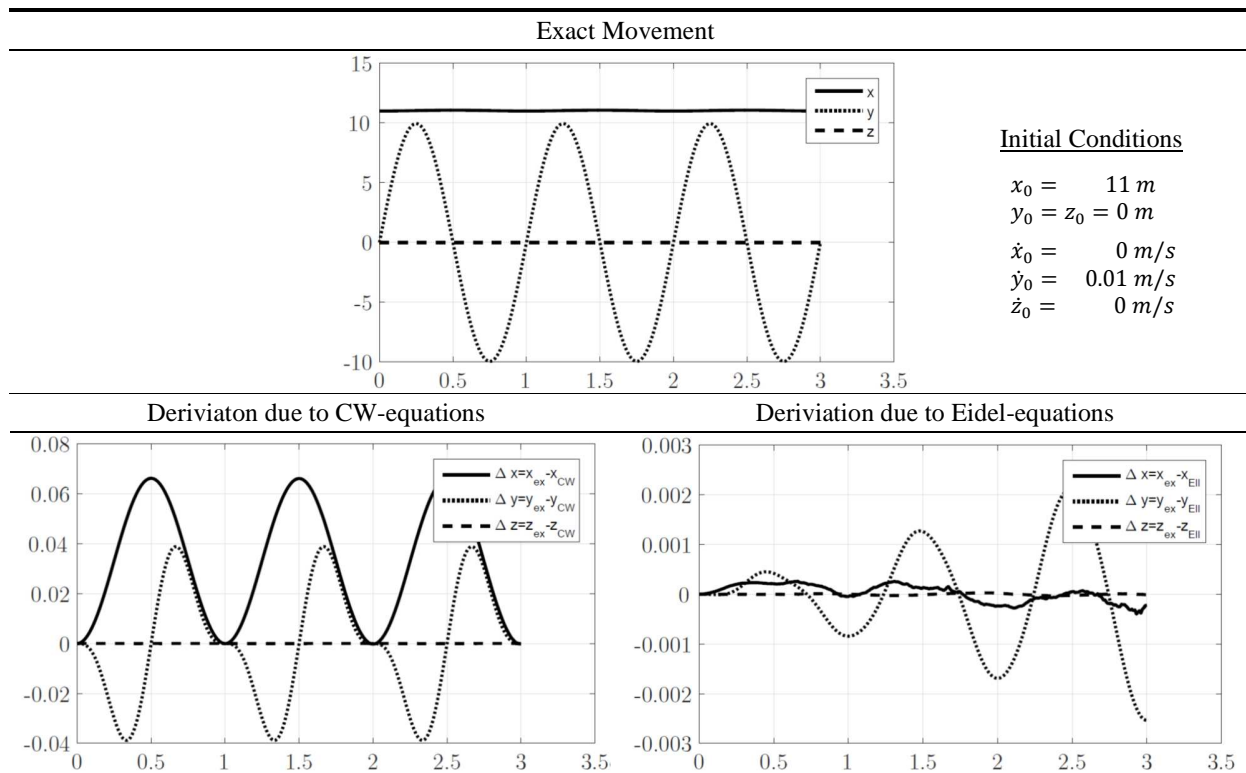
Tab. 3. Relative position due to distance in x-direction



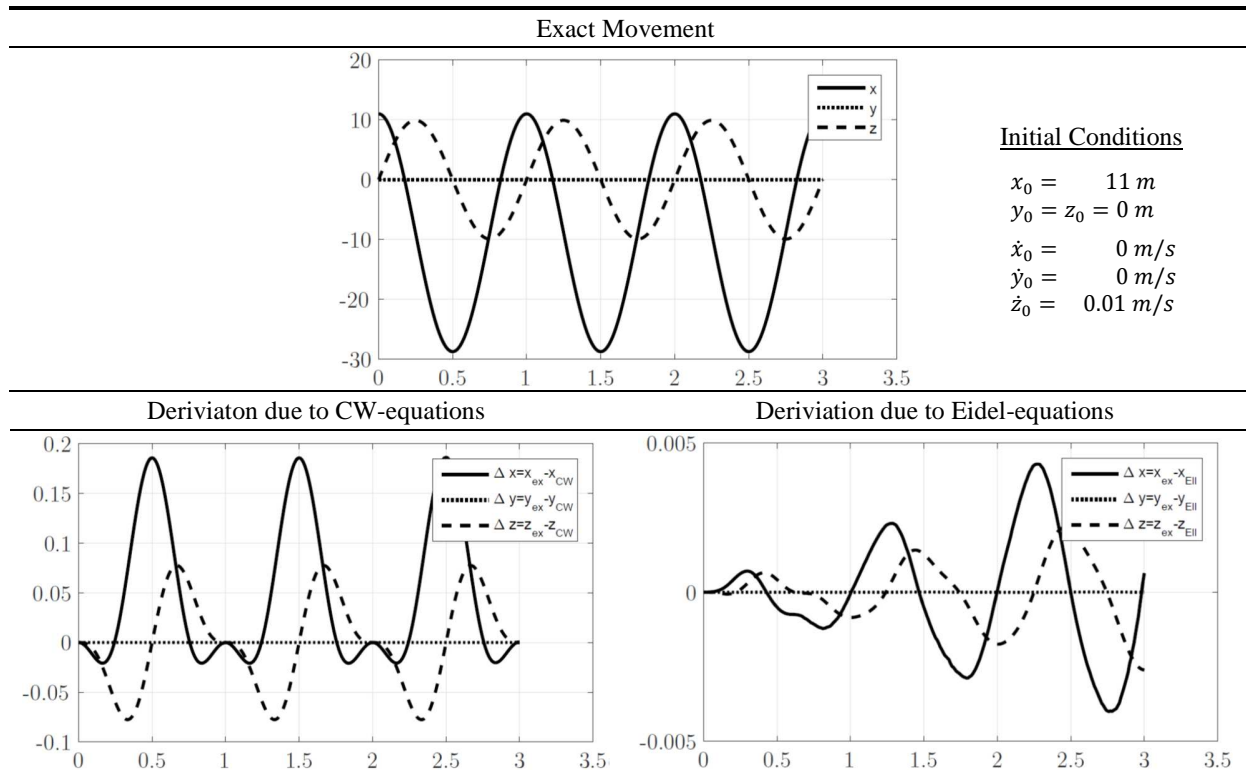
Tab. 4. Relative position due to distance and velocity in x-direction



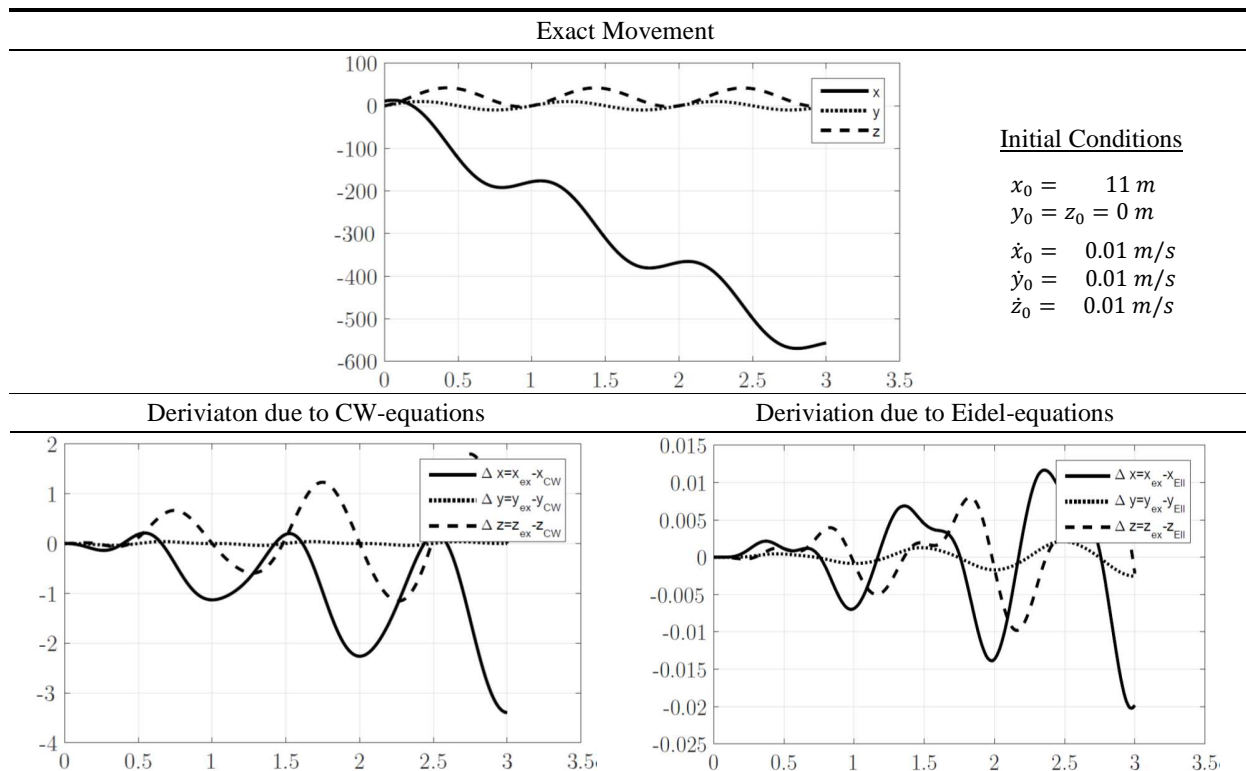
Tab. 5. Relative position due to distance in x- and velocity in y-direction



Tab. 6. Relative position due to distance in x- and velocity in z-direction



Tab. 7. Relative position due to distance in x- and velocity in x-, y-, z-direction



Failure implementation

Failures of spacecraft during a mission are very unpleasant. Any remedial maintenance of the hardware is simply not possible at the moment (which might be changed with on-board servicing). Thus, commands have to be sent in order to hopefully solve an occurring problem. During the approach of an uncooperative target, the switch into safe mode could be hazardous, as the drift could lead to a collision. The implementation of a failure detection, isolation and recovery (FDIR) algorithm is therefore essential for high level autonomy. While different approaches are investigated in other research [13], ADReS-A shall concentrate on the recovery part. Different failures can have similar symptoms. For the success of the mission, it is therefore rather considered to treat those symptoms than to find the fault – at least during the close proximity operations to avoid the risk of collision at any time. A decision has to be made if the failure, or disturbing sensor data, allow for a further approach or require an abort.

Simplifications

DISTURBANCES influencing a satellite's low orbit in space are solar radiation pressure, the gravity-gradient, the flattening of Earth's poles (J2-term), the magnetic field or the satellite's aerodynamic drag. While the solar radiation pressure and the aerodynamic drag highly depend on a satellite cross-section, the gravity gradient and the J2-term influence a space object depending on their position. The magnetic field perturbation depends on a satellite's dipole moment and is usually in the order of $1/4^{\text{th}}$ of the gravitational perturbation. As the target and the chaser set-up have similar geometries, similar mass and are in close vicinity, at least during the simulation run, those disturbances are neglected for the calculations.

The ROBOTIC ARM was set as one spacecraft specification. It shall operate while the chaser stays in the berthing box. Other than power, mass and geometry specifications, based on data provided by the DEOS mission [14], specifications will not be determined. Further research, for example on the actual operation of the arm, will not be performed and is taken as black box.

RELATIVE MOTION in space is highly counter-intuitive. Analytic calculations like the CW-equations or the ones performed by Eidel help understanding those motions. Tab. 4 to Tab. 7 show their deviation from the exact coordinates - the more time passes, the higher the deviation value. Even though Eidel's calculations are more precise by the factor of 35 to 200, the CW-equations only differ by 0.6% from the actual value. Therefore, the equations for small elliptical bodies are not implemented for now.

FAILURES are implemented and can appear any time during the approach. However, a deeper analysis of their origin is not planned. Symptoms will be discussed in a later state of the project. At the time of writing, the implemented failure will defiantly lead to an abort. The decision to be made is now, which trajectory has to be followed that is most fuel saving to allow for multiple approaches.

Safety

As the spacecraft and the rocket body are already idealized as cylinder, they also have a safety area implemented to avoid collision at any time. This area shall not be penetrated by the other object at any time. Following different safety requirements, this area can be adopted in size. The safety area for the simulation is visible in the figures of the following section, as well as results on the propellant consumption for different safety demands.

Connecting points

The simulation is work in progress. While the approach and abort are sufficiently simulated, the failure implementation or autonomy extension are still pending points. Moreover, parts might need to be adopted to changing requirements. Thus, object oriented programming shall be aimed for. Having outsourced files allows for a relatively safe change of parameters, which again will affect the testing itself positively.

4.2 Visualization

Approach

At the time of writing, the simulation uses cylindrical geometry for the target and the main satellite-kit setup. Accordingly, the data used from the design are the dimensions of the respective object, its mass, its propulsion capability and the moments of inertia derived from the preliminary 3D-model created. The approach trajectory is based on the optimization algorithm provided by Gerdts [9] and improved for satellite application by Michael [10], allowing for an approach of a tumbling target, optimized for fuel consumption. Fig. 4 displays the visual outcome.

As predefined by the CW-equations, the center for relative calculations is within the target - the x-, y-, and z-axes are presented by the red, blue and green line. The light blue line shows the approach trajectory, the tripods represent the docking points of the two objects and the yellow line shows their position during the whole approach. As the target

has an angular velocity ω_x of $1^\circ/\text{s}$ and ω_y of $0.5^\circ/\text{s}$, its yellow line forms a circle. The yellow line of the chaser keeps pointing towards its targeted docking point.

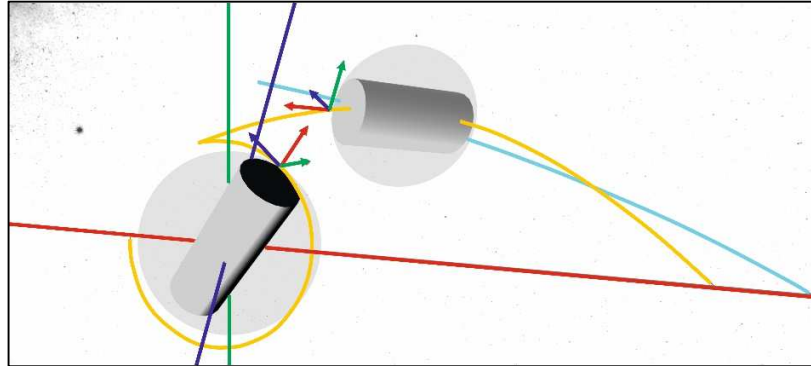


Fig. 4. Approach trajectory incl. safety areas, following [15]

Fig. 5 shows the same approach as Fig. 4, but adds potential abort trajectories, colored as violet lines. These trajectories have been calculated beforehand and use the same optimization algorithm as the approach. The approach trajectory has been discretized into 10 parts, resulting in ten abort trajectories. While an early intervention ends up with the chaser aborting to its starting point, after about 210 s it is considered safer, to aim for the other side of the object. The numbers of are based on an approach time of 9 min. It should be added, that the safety area of the objects adapts according to the trajectory part passed already. The used equation is the following:

$$s_{-}(t, Err) = \max |C_{Err} \cdot |r_{-}^{Err}|, s_{-}t|$$

The closer the chaser gets to the target, the less safety area can be built between the two objects. Therefore, the abort trajectories draw smaller circles around the target the later the failure occurred and thus the further the chaser approached on the trajectory. Fig. 6 shows the according fuel consumption (hydrazine). The black dots show the ten performed steps of Fig. 5, the white dots have been implemented additionally, separating the approach into 20 parts. While the black dotted line displays the result of very high safety margins (C_{err} represents the safety factor added and is a parameter between 1 and 0), a smaller C_{err} is displayed in the gray dotted line. The straight horizontal line shows the propellant consumption without intervention. It will depend on the final safety requirements, which safety parameter is in favor and how much propellant consumption can be approved. The figures also show, that abort trajectories should not be repeated too often due to the high propellant requirements. As the safety parameters can be adapted during the mission, they could be set to smaller values if the mission shows too many required extra approach attempts.

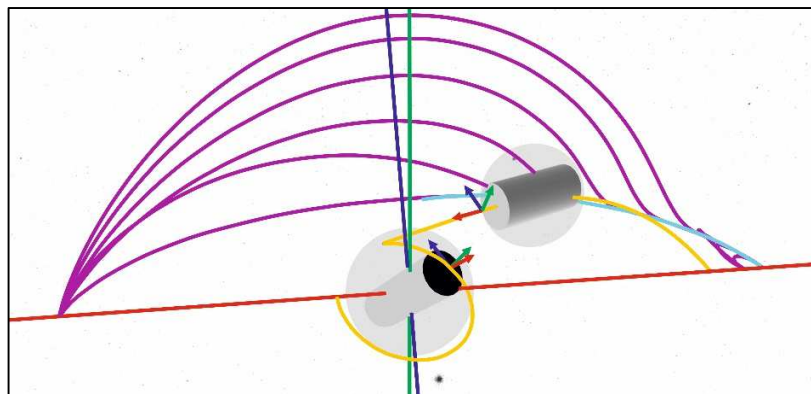


Fig. 5. Approach trajectory and potential abort trajectories, following [15]

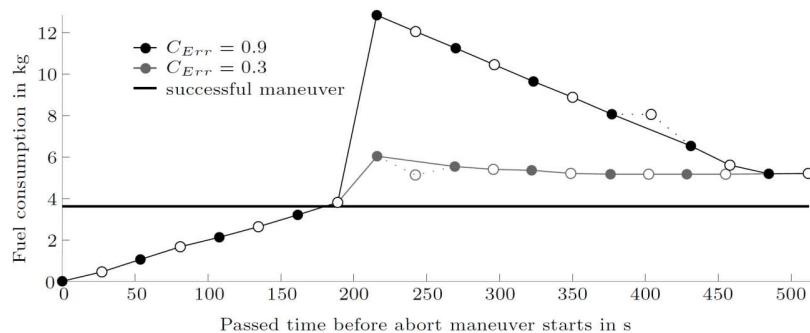


Fig. 6. Fuel consumption for different abort trajectories. The straight line presents the maneuver without abort, following [1]

5. CONCLUSION

Simulations for sufficient testing of autonomous processes in Earth's orbit are work in progress – just as the development of autonomous spacecraft. Active debris removal needs to be encouraged for a safe and stable space environment, thus the simulation presented in this work concentrates on the approach of an uncooperative tumbling target. As simulations have to be adapted to a specific mission, the concept of ADReS-A was first presented. The mission allows for controlled deorbit of SL-8 rocket bodies. Specific parameters of the ADR-missions, such as the size, geometry and mass of the target and the chaser, as well as the environmental circumstances have been implemented. Further considerations on different aspects of the simulation are explained, simplifications are named and intended developments of the model are presented. A first visualization and calculation of trajectories and propellant consumption was presented. Further input will be made in respect to the failure symptom implementations and sensor analysis.

6. ACKNOWLEDGEMENTS

The presented work is supported by Munich Aerospace and Helmholtz Association. The project *Sicherheit im Orbit*, the guiding theme for this work, is a cooperation between DLR and Universität der Bundeswehr München. Additionally, the authors would like to thank Johannes Michael for his support on the simulation implementation and Dr. Eidel for making available his calculations on small eccentricities in Low Earth orbit. Acknowledgments also go to the students of the Universität der Bundeswehr München that supported this work with their theses.

7. REFERENCES

- [1] S. Peters, M. Schöpplein, R. Förstner and H. Fiedler, „Simulation Environment for the Rendezvous Path and Abort Trajectory of ADReS-A,“ in *AIAA Space 2016*, Long Beach, CA, USA, 2016.
- [2] J. C. Liou, „Engineering and Technology Challenges for Active Debris Removal,“ *Progress in Propulsion Physics*, Vol. 4, pp. 735 - 748, 2013.
- [3] C. Bonnal, „Proceedings,“ in *4th International Workshop on Space Debris Modelling and Remediation*, Paris, 2016.
- [4] S. Peters, H. Fiedler, W. Mai and R. Förstner, "Research Issues and Challenges in Autonomous Active Space Debris Removal," in *64th International Astronautical Congress*, Beijing, China, 2013.
- [5] „Aerospace,“ [Online]. Available: <http://www.aerospace.org/cords/spacecraft-reentry/>. [Zugriff am 09 09 2016].
- [6] S. Peters, R. Förstner and H. Fiedler, „Mission Architecture for Active Space Debris Removal using the Example of SL-8 Rocket Bodies,“ in *International Association for the Advancement of Space Safety (IAASS)*, Friedrichshafen, Germany, 2014.

- [7] W. Fehse, "Rendezvous with and Capture/Removal of Non-Cooperative Bodies in Orbit," *Journal of Space Safety Engineering*, vol. 1, no. 1, pp. 17 - 27, 2014.
- [8] H. Gomez Martinez and B. Eissfeller, „Autonomous Determination of Spin Rate and Rotation Axis of Rocket Bodies based on Point Clouds,“ *AIAA Guidance, Navigation, and Control Conference*, 2016.
- [9] M. Gerdts, „Optimal Control and Parameter Identification with Differential-Algebraic Equations of Index 1,“ 2010. [Online]. Available: <http://goo.gl/EofBhP>. [Zugriff am 09 09 2016].
- [10] J. Michael, K. Chudej, M. Gerdts and J. Pannek, „Optimal Rendezvous Path Planning to an Uncontrolled Tumbling Target,“ in *IFAC Proceedings Volumes*, 2013.
- [11] W. Eidel, *Relative Dynamic for small elliptical bodies*, Neubiberg, 2014.
- [12] S. Peters, W. Eidel and R. Förstner, „Architecture and First Achievements of a Simulation for the Approach to an Uncooperative Target,“ in *IEEE Aerospace*, Big Sky, MT, USA, 2017.
- [13] A. Wander and R. Förstner, „Innovative Fault Detection, Isolation and Recovery on-board Spacecraft: Study and Implementation using Cognitive Automation,“ in *2nd International Conference on Control and Fault Tolerant Systems*, 2013.
- [14] P. Rank, Q. Mühlbauer, W. Naumann and K. Landzettel, „The DEOS Automation and Robotics Payload,“ *Acta Astronautica*, Vol. 65, Nr. 1-2, pp. 95-102, 2011.
- [15] M. Schöpplein, „Erstellen einer Simulationsumgebung für das Docking eines Satelliten an ein Weltraumobjekt,“ Neubiberg, Germany, 2015.